Proc. Natl. Acad. Sci. USA
Vol. 86, pp. 9198–9202, December 1989
Biochemistry

Sequence-specific intercalating agents: Intercalation at specific sequences on duplex DNA via major groove recognition by oligonucleotide–intercalator conjugates

(triple helix/fluorescence/acridine derivatives/footprinting/artificial nucleases)

JIAN-SHENG SUN*, JEAN-CHRISTOPHE FRANÇOIS*, THÉRÈSE MONTENAY-GARESTIER*, TULA SAISON-BEHMOARAS*, VICTORIA ROIG†, NGUYEN T. THUONG†, AND CLAUDE HÉLÈNE*

*Laboratoire de Biophysique, Muséum National d'Histoire Naturelle, Institut National de la Santé et de la Recherche Médicale, Unité 201, Centre National de la Recherche Scientifique, Unité Associée 481, 43, Rue Cuvier, 75231 Paris Cedex 05, and †Centre de Biophysique Moléculaire, Centre National de la Recherche Scientifique, 45071 Orléans Cedex 02, France

Communicated by Gary Felsenfeld, August 30, 1989 (received for review May 1, 1989)

ABSTRACT **An acridine derivative was covalently linked to the 5′ end of a homopyrimidine oligonucleotide. Specific binding to a homopurine·homopyrimidine sequence of duplex DNA was demonstrated by spectroscopic studies (absorption and fluorescence) and by "footprinting" experiments with a copper phenanthroline chelate used as an artificial nuclease. A hypochromism and a red shift of the acridine absorption were observed. Triple-helix formation was also accompanied by a hypochromism in the ultraviolet range. The fluorescence of the acridine ring was quenched by a stacking interaction with a G·C base pair adjacent to the homopurine·homopyrimidine target sequence. The intercalating agent strongly stabilized the complex formed by the oligopyrimidine with its target duplex sequence. Cytosine methylation further increased the stability of the complexes. Footprinting studies revealed that the oligopyrimidine binds in a parallel orientation with respect to the homopurine-containing strand of the duplex. The intercalated acridine extended by 2 base pairs the region of the duplex protected by the oligopyrimidine against degradation by the nuclease activity of the copper phenanthroline chelate. Random intercalation of the acridine ring was lost due to the repulsive effect of the negatively charged oligonucleotide tail. Intercalation occurred only at those double-stranded sequences where the homopyrimidine oligonucleotide recognized the major groove of duplex DNA.**

The selective recognition of nucleic acid base sequences plays a central role in molecular biology. Gene expression is controlled by sequence-specific regulatory proteins such as repressors or activators. Several such proteins have been shown to recognize the major groove of DNA (1). By contrast, many DNA-binding drugs bind to the minor groove (2). Intercalating agents usually bind via the minor groove (3), even though there are reported cases in which intercalation occurs from the major groove (4).

Watson–Crick base pairs in DNA still possess several hydrogen bonding sites that are accessible in both the major and minor grooves (1). In the major groove, thymine can form two hydrogen bonds with an adenine involved in a Watson–Crick A·T base pair. Protonated cytosine can also form two hydrogen bonds with a guanine engaged in a Watson–Crick G·C base pair. It is thus possible to form local triple helices with two polypyrimidine strands hydrogen bonded to a corresponding polypurine (5–9). The third (polypyrimidine) strand is bound to the major groove of the Watson–Crick duplex. We previously showed that an oligothymidylate could bind to the major groove of a DNA fragment at an $(A)_n \cdot (T)_n$ sequence (10, 11). When the oligothymidylate carried a photoactive group at one end, it was possible to photocrosslink the oligonucleotide to each strand of the double helix (10, 11). The location of the crosslinked sites allowed us to demonstrate that the oligothymidylate was bound in a parallel orientation with respect to the homopurine-containing strand of the duplex. Sequence-specific recognition of the major groove of DNA by oligodeoxypyrimidylates containing both cytosines and thymines was also demonstrated by a "footprinting" technique in which copper phenanthroline chelate was used as a cleaving reagent (12). Moser and Dervan (13) showed that cleavage reactions could be targeted to specific homopurine·homopyrimidine tracts of double-stranded DNA using an EDTA Fe chelate tethered to an oligopyrimidylate. Double-strand cleavage could also be induced by a copper phenanthroline chelate tethered to an oligopyrimidine (14).

We previously synthesized oligodeoxynucleotides covalently linked to an intercalating agent (15–18). These compounds were shown to bind more strongly than the unsubstituted oligonucleotide to a single-stranded nucleic acid containing the complementary sequence. This was ascribed to an additional binding energy provided by interaction of the intercalating agent with the duplex structure formed by the oligonucleotide with its complementary sequence. Here we show that a homopyrimidine oligodeoxynucleotide whose 5′ end was covalently linked to an acridine derivative behaves as a sequence-specific DNA intercalating agent. The oligonucleotide binds to a specific sequence in the major groove of the duplex, thereby forming a triple helix. The acridine intercalates at the triplex–duplex junction and stabilizes the complex. In addition, we show that random intercalation of the acridine with duplex DNA is abolished by the negatively charged oligonucleotide chain attached to it. Therefore, intercalation can take place only at those sequences where the homopyrimidine oligonucleotide finds a target homopurine·homopyrimidine sequence.

MATERIALS AND METHODS

Oligonucleotide Synthesis. Two sets of complementary DNA fragments 32 nucleotides long were synthesized on a Pharmacia automatic synthesizer by phosphoramidite chemistry. Their sequences are shown on Fig. 1. Attachment of the acridine derivative to the 5′ side of the 11-mer oligodeoxy-

The publication costs of this article were defrayed in part by page charge payment. This article must therefore be hereby marked "*advertisement*" in accordance with 18 U.S.C. §1734 solely to indicate this fact.

Abbreviations: t_m, melting temperature (°C); 11β(p), unsubstituted 11-mer homopyrimidylate; 11β^{m}C(p), 11-mer oligodeoxypyrimidylate in which cytosines are replaced by 5-methylcytosines; Acr-11β(p), 11-mer homopyrimidylate with acridine linked covalently to its 5′ end; AcrOH, 2-methoxy-6-chloro-9-aminoacridine with a hydroxypentamethylene substituent attached to the 9-amino group.

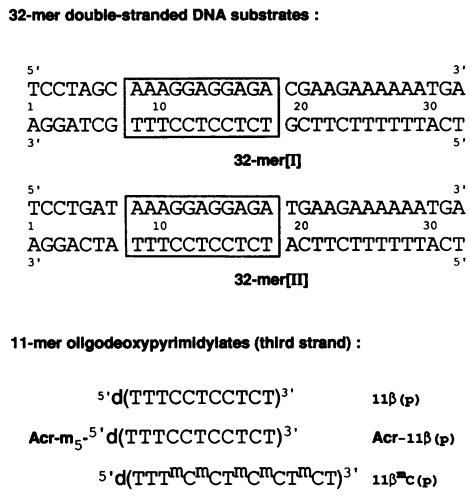

FIG. 1. Sequences of the two 32-mer double-stranded DNA substrates and three 11-mer oligodeoxypyrimidylates (third strand) used in the present work. All 11-mer oligodeoxynucleotides were synthesized in parallel orientation with respect to the homopurine strand of the duplex. Boxes represent the site for triple-helix formation. The intercalating agent, 2-methoxy-6-chloro-9-aminoacridine (Acr), is attached to the 5'-phosphate of the oligodeoxynucleotide via a pentamethylene linker (m_5).

nucleotide was achieved by solid-phase synthesis using the phosphoramidite derivative of 2-methoxy-6-chloro-9-(ω-hydroxylpentylamino)acridine as described (19). All synthesized oligonucleotides were purified by HPLC on Mono Q HR 5/5 Pharmacia columns followed by gel electrophoresis. The following chemicals were obtained from commercial sources: 1,10-phenanthroline (Merck), 2,9-dimethyl-1,10-phenanthroline, copper sulfate, 3-mercaptopropionic acid (Janssen Chemica), spermine (Sigma), and ethylene glycol (Prolabo, Paris).

All solutions were prepared in a buffer containing 10 mM sodium cacodylate and various concentrations of NaCl or spermine. The 32-mer duplex was prepared in the buffer by annealing the homopurine-containing strand with an excess of the homopyrimidine-containing strand (ratio, ≈1.5) to ensure that there was no free homopurine-containing single strand at room temperature. No interaction between the 11-mer oligodeoxypyrimidylates and the homopyrimidine-containing single strand was observed in our study.

Spectroscopic Methods. Absorption spectra were recorded on a Uvikon 820 spectrophotometer (Kontron, France) using quartz suprasil microcells of a 1-cm optical pathway. Fluorescence spectra were recorded on a Spex Fluorolog FIT11 spectrofluorometer (Spex Industries, Edison, NJ). They were corrected for the wavelength dependence of the transmission and detection systems. The areas under the fluorescence spectra were then calculated to obtain relative fluorescence quantum yields. The excitation wavelength was 424 nm. During spectroscopic experiments, the temperature was controlled with a thermostated cell holder and a Haake D8G thermostat equipped with a Haake PG10 temperature programer. The melting profiles were recorded by increasing the temperature at a rate of 0.1°C/min. The absorbance vs. temperature curves were also recorded upon cooling the samples to check the reversibility of the process, which proved to be good in all cases. Melting temperatures (t_m) were taken as the temperatures corresponding to half-dissociation of the complexes, and the reproducibility of t_m was ±0.5°C. The fluorescence melting profiles were obtained by measuring the relative fluorescence quantum yield of the acridine-substituted oligonucleotide in the presence and absence of duplex at each temperature (20).

Footprinting by Copper Phenanthroline. The conditions for footprinting experiments have been described (12). In a typical experiment, the 32-mer duplex (10 nM) was incubated with 1,10-phenanthroline (10 μM), $CuSO_4$ (2.5 μM), and 2-mercaptopropionic acid (2 mM). The oligopyrimidines were added at 5 μM. The reaction was carried out at 0°C for 1 hr in a pH 6 buffer containing 10 mM phosphate, 0.1 M NaCl, 1 mM spermine, and 20% (vol/vol) ethylene glycol. One of the 32-mer strands was 5'-end-labeled with [γ-^{32}P]-ATP and polynucleotide kinase (Amersham). After the reaction, samples were loaded on 20% polyacrylamide gel and electrophoresed for 2 hr at 20°C. Autoradiograms were obtained by exposing the gels to Kodak or Fuji (x-ray) films at −20°C. Densitometric methods were used to analyze the cleavage pattern induced by $Cu(OP)_2$ on the 32-mer duplex in the absence or presence of oligopyrimidines. Microdensitometry of autoradiograms was performed on a LKB laser densitometer interfaced with a compatible PC microcomputer (Olivetti).

RESULTS

Absorption. The temperature dependence of the ultraviolet absorption of mixtures of the 32-mer[I] double-stranded DNA fragment with the 11-mer oligodeoxypyrimidylates [11β(p), the unsubstituted homopyrimidylate; 11β^{m}C(p), oligodeoxypyrimidylate in which 5-methylcytosine replaces cytosine; or Acr-11β(p), acridine-substituted oligodeoxypyrimidylate] was measured at 258 nm in the presence of different cations. Thermal dissociation curves presented two transitions in the presence of either high NaCl concentrations or low concentrations of a polycation such as spermine. The transition occurring in the upper temperature range (>60°C) was observed in the absence of any 11-mer oligonucleotide and was therefore attributed to the thermal dissociation of the 32-mer duplex. The transition in the lower temperature range was not observed in the absence of the 11-mer and was therefore ascribed to the thermal dissociation of a complex formed by the 11-mer oligopyrimidylate with the 32-mer duplex. Fig. 2 shows the derivative of the melting curves for this transition recorded at 258 nm.

Triple-helix formation could also be observed in the visible range at 424 nm in the absorption band of 2-methoxy-6-chloro-9-aminoacridine covalently linked to the 11-mer oligodeoxypyrimidylate (Fig. 3*A*). Triple-helix formation was characterized by a hypochromism at 424 nm and a red shift of the absorption band with an isosbestic point at 458 nm.

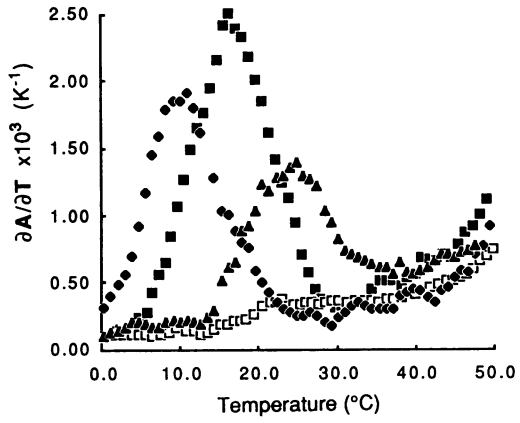

FIG. 2. Derivatives of the optical transition curves in the low temperature range, obtained by measurement of absorbance at 258 nm as a function of temperature: □, 32-mer only; ◆, 32-mer + 11β(p); ■, 32-mer + 11β^{m}C(p); ▲, 32-mer + Acr-11β(p). The 11-mer oligodeoxypyrimidylates and 32-mer duplex were equimolar (1 μM) in a buffer containing 10 mM sodium cacodylate/1 M NaCl at pH 6.

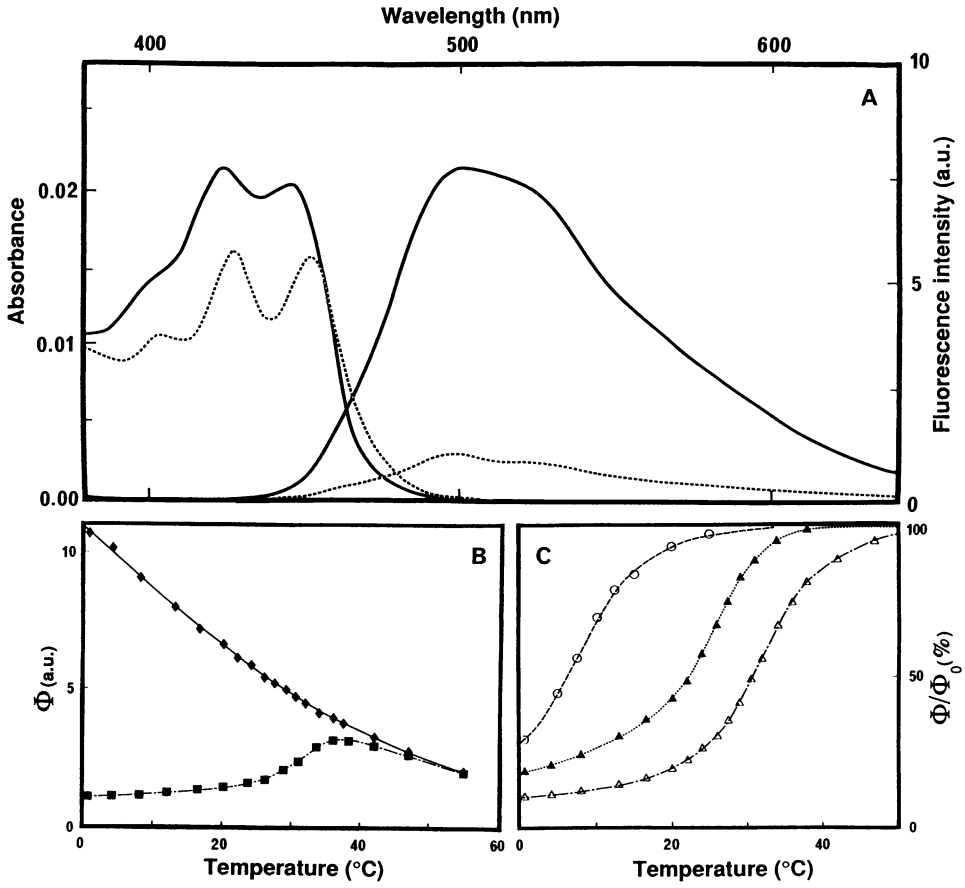

FIG. 3. (*A*) Visible absorption and fluorescence emission of the free Acr-11β(p) (solid line) and the triplex 32-mer + Acr-11β(p) (dotted line). The Acr-11β(p) and 32-mer were equimolar ($\approx$2.2 μM) in the buffer containing 1 M NaCl and 10 mM sodium cacodylate (pH 6) at 0°C. Excitation was at 424 nm for emission measurements. (*B*) Temperature dependence of the relative fluorescence quantum yield of free Acr-11β(p) (◆) and the triplex 32-mer + Acr-11β(p) (■). Fluorescence measurements were carried out the same as in *A*. (*C*) Temperature dependence of the ratio between the fluorescence yield of the triplex 32-mer + Acr-11β(p) and that of the free Acr-11β(p). The curves were obtained at 0.1 M NaCl (pH 6) (▲), 1 M NaCl (pH 6) (△), and 1 M NaCl (pH 7) (○). a.u., Arbitrary units.

This behavior was previously observed when the acridine derivative intercalates into DNA (16, 21). The thermal dissociation curve observed at 424 nm was identical to that obtained at 258 nm.

The thermal stability of the triple helix was characterized by its t_m (Table 1). The intercalating agent linked covalently to the 11-mer homopyrimidylate [Acr-11β(p)] strongly stabilized the triplex structure. The t_m was increased by 13°C–18°C depending on the salt conditions (see Table 1). As shown in Table 1, the t_m of the acridine-substituted 11-mer was 37.4°C in the pH 6 buffer in the presence of 0.1 M NaCl and 1.0 mM spermine. The total oligonucleotide concentration was 1 μM. Therefore, the equilibrium constant for triple-helix formation was $\approx 2 \times 10^6$ M^{-1} at 37°C. The t_m of triplexes involving the 11-mer oligodeoxypyrimidylate 11β^mC(p) was 5°C–9°C higher than that of 11β(p). Binding was pH dependent as expected because cytosines must be protonated to form Hoogsteen hydrogen bonds with a Watson–Crick G·C base pair. The t_m for Acr-11β(p) was decreased by $\approx$10°C when the pH was increased from 6 to 7 in the presence of 0.1 M NaCl.

Table 1. t_m ($\pm$0.5°C) of the different triplex–duplex equilibria

Triplex	NaCl, M	Spermine, mM	t_m, °C
32-mer + 11β(p)	0.1	0.1	13.9
	0.1	1.0	19.3
	1.0	—	11.4
32-mer + 11β^mC(p)	0.1	0.1	21.3
	0.1	1.0	28.8
	1.0	—	16.6
32-mer + Acr-11β(p)	0.1	0.1	27.6
	0.1	1.0	37.4
	1.0	—	24.3

For t_m measurements, 11-mer oligodeoxypyrimidylates and 32-mer duplex were equimolar (1 μM) in the pH 6 buffer containing 10 mM sodium cacodylate and NaCl or spermine as indicated.

Fluorescence. The fluorescence properties of the intercalating agent were used to investigate triple-helix formation. The fluorescence of acridine derivatives is sensitive to their environment (22). The fluorescence of 2-methoxy-6-chloro-9-aminoacridine is enhanced when the acridine ring is intercalated between A·T base pairs. In contrast, its fluorescence is strongly quenched when the acridine ring is in contact with a G·C base pair (22). Two G·C base pairs are adjacent to the 5′ side of the homopurine·homopyrimidine tract in the 32-mer[I] double-stranded DNA fragment. When Acr-11β(p) binds in a parallel orientation with respect to the homopurine sequence in the 32-mer[I] duplex, the acridine ring is brought in the immediate vicinity of G·C base pairs. If intercalation takes place at the triplex–duplex junction, its fluorescence is expected to be strongly quenched.

As shown in Fig. 3, the fluorescence of Acr-11β(p) was strongly quenched upon binding to the homopurine·homopyrimidine tract of the 32-mer[I] duplex. Fluorescence quenching was $\approx$90% at 0°C in the pH 6 buffer. Upon increasing the temperature, the fluorescence of Acr-11β(p) decreased monotonically in the absence of duplex. In contrast, an increase was first observed for the triple-helix complex followed by a decrease (Fig. 3*B*). At high temperature, the fluorescence was identical to that of the free Acr-11β(p). The relative fluorescence quantum yield as a function of temperature is shown in Fig. 3*C* at different monocationic salt concentrations. Cooperative melting curves were obtained that gave the same t_m as obtained in the absorption studies.

Nonspecific Binding of the Acridine-Substituted Oligonucleotide. Acridine derivatives such as 2-methoxy-6-chloro-9-aminoacridine are nonspecific intercalating agents (21). They bind equally well at A·T and G·C base pairs. Attachment

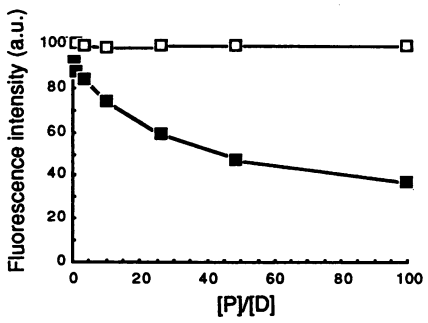

FIG. 4. Titration of the intercalator–linker conjugate AcrOH (8 μM; ■) and the intercalator–linker–oligonucleotide conjugate Acr-11β(p) (8 μM; □) by calf thymus double-stranded DNA followed by fluorescence emission (λ_{exc} = 424 nm, λ_{em} = 498 nm) in the pH 6 buffer containing 10 mM sodium cacodylate and 1 M NaCl at 0°C. a.u., Arbitrary units; [P]/[D], phosphate/dye ratio.

of an oligonucleotide to the 9-aminoacridine derivative should strongly affect this nonspecific intercalation. Repulsive forces between the negatively charged oligonucleotide "tail" and duplex DNA should prevent intercalation at sites where the oligonucleotide does not find a target sequence. We have compared the DNA binding of 2-methoxy-6-chloro-9-aminoacridine carrying a hydroxypentamethylene substituent attached to the 9-amino group (abbreviated Acr-OH), and 2-methoxy-6-chloro-9-aminoacridine coupled to the 11-mer homopyrimidylate using the same pentamethylene linker [Acr-11β(p)]. Fig. 4 shows the fluorescence titration curve of AcrOH and Acr-11β(p) by calf thymus double-stranded DNA in 10 mM sodium cacodylate buffer (pH 6) containing 1 M sodium chloride at 0°C. The fluorescence observed at 498 nm was quenched when AcrOH was titrated by increasing amounts of calf thymus DNA. In contrast, no quenching was observed during the titration of Acr-11β(p) by calf thymus DNA, indicating that acridine has lost its nonspecific intercalation properties when covalently attached to the oligonucleotide.

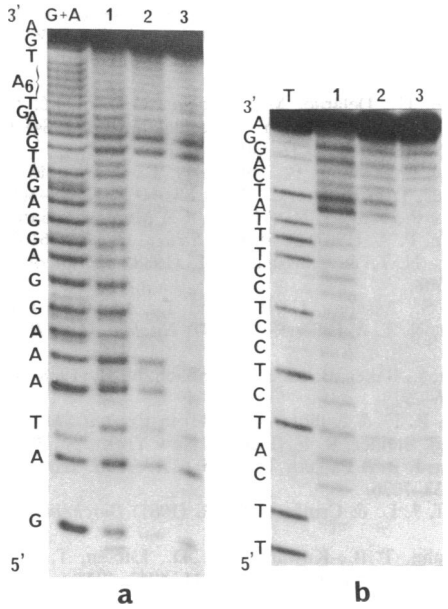

FIG. 5. Footprinting studies on the 32-mer[II] duplex using copper phenanthroline as a cleaving reagent. (*a*) The purine-rich strand was 5'-end-labeled. The G+A sequence is shown in the left lane. (*B*) The pyrimidine-rich strand was 5'-end-labeled, and the left lane represents the T sequence. Cleavage was carried out in the absence (lane 1) or in the presence of the unsubstituted 11-mer (lane 2) and the acridine-substituted 11-mer (lane 3).

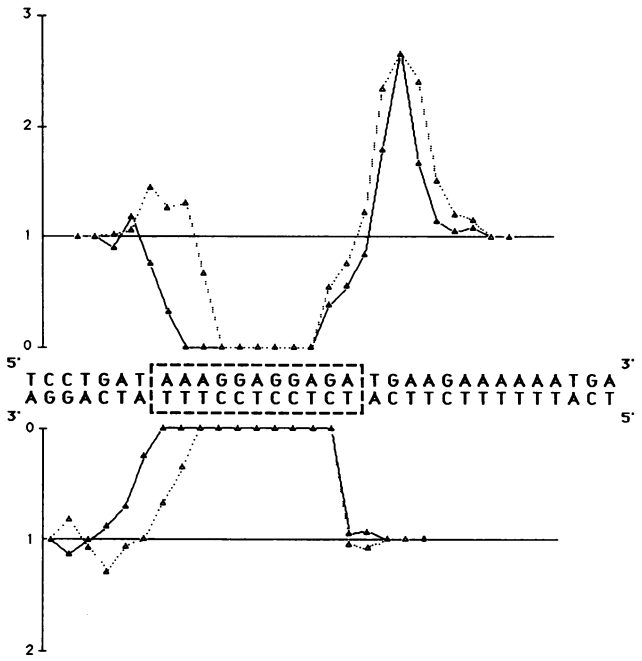

FIG. 6. Quantitative analysis of the cleavage pattern as described in ref. 12. The ratio of the cleavage efficiency in the presence and absence of the oligonucleotide is shown above the sequence for the purine-containing strand and below the sequence for the pyrimidine-containing strand. A value of 1 means that cleavage was not altered by the oligonucleotide; a value of 0 means full protection. Dotted lines (open symbols) correspond to the unsubstituted 11-mer. Solid lines (solid symbols) correspond to the acridine-substituted 11-mer.

Footprinting Studies. To obtain more information on the structure of the complexes formed by the acridine-substituted 11-mer with the 32-mer duplex, its footprint was compared to that of the unsubstituted 11-mer. We have previously reported that the copper phenanthroline chelate could be used as an artificial nuclease to reveal the binding of an oligonucleotide to the major groove of DNA (12) (Fig. 5). A footprint was observed on both strands of duplex DNA, reflecting the protection against nuclease degradation afforded by oligonucleotide binding. As shown in Fig. 6, there is a clear difference between the footprints observed in the absence and in the presence of the acridine substituent. The changes are located on the 5' side of the homopurine sequence and on the 3' side of the homopyrimidine sequence, indicating that the acridine is located where expected if the 11-mer oligopyrimidylate binds in a parallel orientation with respect to the homopurine-containing strand.

A quantitative analysis of the footprints was carried out. The ratio of the intensities of the cleaved fragments in the presence and in the absence of the oligopyrimidylate is plotted in Fig. 6. There is no marked difference between the unsubstituted and the acridine-substituted 11-mer footprints on the 3' side of the oligonucleotide. In contrast, the footprint is shifted by 2 base pairs on the 5' side of the oligonucleotide when the latter carries the acridine substituent. Similar results were obtained with the two 32-mers ([I] and [II]).

DISCUSSION

A homopyrimidine oligodeoxynucleotide covalently linked via its 5'-phosphate to an acridine derivative binds to the major groove of duplex DNA at a homopurine·homopyrimidine sequence. The stability of the triple-stranded complex is strongly increased as compared to the unsubstituted oligonucleotide. Spectroscopic results are in agreement with an intercalation of the acridine ring at the triplex–duplex

junction. First, the hypochromism and the red shift of the visible absorption band of the acridine derivative are similar to the properties observed for intercalated acridine. Second, the fluorescence of acridine is strongly quenched, indicating that the acridine ring is engaged in stacking interactions with guanine in a G·C base pair. A G·C base pair is indeed adjacent to the triplex structure. Third, model building studies show that the pentamethylene linker allows for intercalation at the junction between the last C·G base pair of the duplex and the first A·T base pair of the T·A·T triplet in the triple-stranded region. It should be remembered that triple helices provide only weak binding sites for intercalating agents as compared to double helices (23, 24). In addition, the pyrimidine 3′–5′ purine step, which is adjacent to the triple helix, is a favored sequence for intercalation (3). Attachment of acridine to the 3′-phosphate of the oligonucleotide via a pentamethylene linker did not induce a strong stabilization (unpublished data). This probably reflects the weak potential for intercalation of the purine 3′–5′ pyrimidine sequence at the triplex–duplex junction on the 3′ side of the bound oligonucleotide.

The footprinting data are also in agreement with intercalation of the acridine ring. Binding of a homopyrimidine oligonucleotide to the major groove of DNA prevents cleavage by the artificial nuclease $Cu(OP)_2$(12). The triplex–duplex junction on the 3′ side of the oligonucleotide has a perturbed structure as revealed by an enhanced cleavage of the homopurine-containing strand when compared to the unbound duplex structure (12). On the contrary, the junction on the 5′ side of the bound oligonucleotide does not exhibit any strong perturbation as compared to duplex DNA. There is still some debate as to the mechanism of $Cu(OP)_2$ binding to DNA. Sigman and co-workers (25) favor minor groove binding. Results from other laboratories were accounted for by intercalation of one of the phenanthroline rings (26, 27). The footprinting data reported in the present study are more satisfactorily explained with the intercalation model. If the acridine tethered to the oligonucleotide is intercalated at the triplex–duplex function, then phenanthroline intercalation should be prevented at the same site and at the adjacent one owing to the nearest-neighbor exclusion that characterizes intercalating substances (3). The footprinting experiments show that the cleavage sites produced by $Cu(OP)_2$ are indeed shifted by 2 base pairs when the oligonucleotide carries the acridine derivative.

Binding of the homopyrimidine oligonucleotide to duplex DNA is salt and pH dependent. The stabilization at acidic pH is due to cytosine protonation, which is required to form C·G·C triplets. The role of cations is more complex. The double helix is a polyelectrolyte that condenses cations, including protons, in its vicinity. The local pH is therefore lower in the immediate proximity of the duplex, which favors cytosine protonation. An increase in Na^+ concentration decreases the local H^+ concentration, which decreases cytosine protonation and, therefore, oligonucleotide binding. On the other hand, an increase in bulk Na^+ concentration should decrease the electrostatic repulsion between the oligonucleotide and the duplex. At pH 6, an increase of NaCl concentration from 0.1 to 1 M in the absence of spermine increased t_m by 8°C, indicating that electrostatic effects are more important than local pH changes.

Methylation of cytosine in a homopyrimidine oligodeoxynucleotide enhances the stability of the complex formed with a double-stranded sequence. Such an effect was previously observed for polynucleotides. Poly[d(T^mC)] forms a more stable triple helix with poly[d(AG)] than unmethylated poly[d(TC)] (6). A similar result was recently reported for oligonucleotides carrying an iron–EDTA chelate (28). This stabilization might be due to a slight shift of the cytosine pK to higher values and to hydrophobic effects.

The present study has shown that it is possible to make intercalating agents sequence specific by attachment to a homopyrimidine oligonucleotide. The negatively charged oligonucleotide tail prevents random intercalation as a result of electrostatic repulsion with duplex DNA. Intercalation takes place only at sites where the oligonucleotide can bind to the DNA major groove by forming a local triple helix. An association constant of $2 \times 10^6\ M^{-1}$ was measured at 37°C and pH 6. Binding can be increased by using longer oligonucleotide sequences and by cytosine methylation. Homopurine oligonucleotides might also form triple helices that are independent of pH (29, 30). Further studies should indicate the sequence requirements necessary to optimize major groove recognition under physiological conditions. The design of sequence-specific DNA intercalating agents opens new possibilities to interfere with biological processes such as replication and transcription.

We thank L. Perrouault for purification and characterization of the oligonucleotides used in this work. This work was supported in part by the Ligue Nationale Française contre le Cancer and Rhône-Poulenc Santé.

1. Hélène, C. & Lancelot, G. (1982) *Prog. Biophys. Mol. Biol.* **39**, 1–68.
2. Zimmer, C. & Wähnat, U. (1986) *Prog. Biophys. Mol. Biol.* **47**, 31–112.
3. Neidle, S. & Abraham, Z. (1984) *C.R.C. Crit. Rev. Biochem.* **17**, 73–121.
4. Delbarre, A., Delepierre, M., Garbay, C., Igolen, J., Le Pecq, J. B. & Roques, B. P. (1987) *Proc. Natl. Acad. Sci. USA* **84**, 2155–2159.
5. Arnott, S. & Selsing, E. (1974) *J. Mol. Biol.* **88**, 509–521.
6. Lee, J. S., Woodsworth, M. L., Latimer, L. J. P. & Morgan, A. R. (1984) *Nucleic Acids Res.* **12**, 6603–6614.
7. Felsenfeld, G., Davies, A. & Rich, A. (1965) *J. Am. Chem. Soc.* **79**, 2023–2024.
8. Riley, M., Maling, B. & Chamberlin, M. J. (1966) *J. Mol. Biol.* **20**, 359–389.
9. Morgan, A. R. & Wells, R. D. (1968) *J. Mol. Biol.* **37**, 63–80.
10. Le Doan, T., Perrouault, L., Praseuth, D., Habhoub, N., Decout, J. L., Thuong, N. T. & Hélène, C. (1987) *Nucleic Acids Res.* **15**, 7749–7760.
11. Praseuth, D., Perrouault, L., Le Doan, T., Chassignol, M., Thuong, N. T. & Hélène, C. (1988) *Proc. Natl. Acad. Sci. USA* **85**, 1349–1353.
12. François, J. C., Saison-Behmoaras, T. & Hélène, C. (1988) *Nucleic Acids Res.* **16**, 11431–11440.
13. Moser, H. E. & Dervan, P. B. (1987) *Science* **238**, 645–650.
14. François, J. C., Saison-Behmoaras, T., Chassignol, M., Thuong, N. T. & Hélène, C. (1988) *C.R. Acad. Sci. Ser. 3* **307**, 849–854.
15. Asseline, U., Thuong, N. T. & Hélène, C. (1983) *C.R. Acad. Sci. Ser. 3* **297**, 369–372.
16. Asseline, U., Delarue, M., Lancelot, G., Toulmé, F., Thuong, N. T., Montenay-Garestier, T. & Hélène, C. (1984) *Proc. Natl. Acad. Sci. USA* **81**, 3297–3301.
17. Asseline, U., Toulmé, F., Thuong, N. T., Delarue, M., Montenay-Garestier, T. & Hélène, C. (1984) *EMBO J.* **3**, 795–800.
18. Cieplak, P., Rao, S. N., Hélène, C., Montenay-Garestier, T. & Kollman, P. A. (1987) *J. Biomol. Struct. Dyn.* **5**, 361–382.
19. Thuong, N. T. & Chassignol, M. (1988) *Tetrahedron Lett.* **29**, 5905–5908.
20. Sun, J. S., Asseline, U., Rouzaud, D., Montenay-Garestier, T., Thuong, N. T. & Hélène, C. (1987) *Nucleic Acids Res.* **15**, 6149–6158.
21. Reuben, J., Baker, B. M. & Kallenbach, N. R. (1978) *Biochemistry* **17**, 2916–2919.
22. Steiner, R. F. & Kubota, Y. (1983) in *Excited States of Biopolymers*, ed. Steiner, R. F. (Plenum, New York), pp. 203–254.
23. Le Pecq, J. B. & Paoletti, C. (1965) *C.R. Hebd. Seances Acad. Sci.* **260**, 7033–7036.
24. Bresloff, J. L. & Crothers, D. M. (1981) *Biochemistry* **20**, 3547–3553.
25. Thederahn, T. B., Kuwabara, M. D., Larsen, T. A. & Sigman, D. S. (1989) *J. Am. Chem. Soc.* **111**, 4941–4946.
26. Williams, L. D., Thivierge, J. & Goldberg, I. H. (1988) *Nucleic Acids Res.* **16**, 11607–11615.
27. Veal, J. M. & Rill, R. L. (1989) *Biochemistry* **28**, 3243–3250.
28. Povsic, T. J. & Dervan, P. B. (1989) *J. Am. Chem. Soc.* **111**, 3059–3061.
29. Cooney, M., Czernuszewicz, G., Postel, E. H., Flint, S. J. & Hogan, M. E. (1988) *Science* **241**, 456–459.
30. Letai, A. G., Palladino, M. A., Fromm, E., Rizzo, V. & Fresco, J. R. (1988) *Biochemistry* **27**, 9108–9112.